Kinetics of N-Deacetylation of Chitin Extracted from Shrimp Shells Collected from Coastal Area of Morocco

Hammou Ahlafi*[1], Hamou Moussout[1], Fatima Boukhlifi[2], Mostafa Echetna[1],
Mohamed Naciri Bennani[1] and Slimani My Slimane[1]

[1]Equipe des Matériaux et Catalyse Appliqués, Laboratoire de Chimie - Biologie Appliquées à l'Environnement, Faculté des Sciences, Meknès, Maroc

[2]Equipe des Matériaux, Métallurgie et Ingénierie des Procédés, Ecole Nationale Supérieure d'Arts et Métiers, Meknès, Maroc

Abstract: Chitosan was obtained from the alkaline N-deacetylation of α-chitin, derived from shrimp shells (SS) collected from the Moroccan coast. Effects of temperature, NaOH concentration and reaction time on the kinetics of deacetylation were studied. The degree of deacetylation (DD = 75%) was obtained at T = 120 °C and C_{NaOH} = 12N in a single step for 6h. It was found, from FTIR studies, that the removal of acetyl groups from chitin occur very fast for the reaction time t < 180 min and then becomes constant after, revealing two steps in the deacetylation of chitin following a first-order kinetics for each of them. The second step is considered the limiting step that has, in the temperature range of 25 – 120 °C and maintained C_{NaOH} = 12N, a low apparent rate constant. The activation energy of this step is about 48.76 kJ/mol. The biopolymer (Chitin and chitosan) produced were characterized by X-ray diffraction.

Key words: chitin, chitosan, N-deacetylation, FTIR spectra, degree of deacetylation, kinetics.

Introduction

Chitin is a polysaccharide corresponding to linear copolymers of β (1→4)-linked 2-amino-2-deoxy-D-glucan and 2-acetamido-2-deoxy-D-glucan, usually isolated from the exoskeletons of crustaceans and more particularly from shrimps, squid pens and crabs. Chitin, especially its main derivative chitosan, has special characteristics such as hydrophilicity, biocompatibility, biodegradability and non-toxicity. These properties offer to these biopolymers a wide range of applications; for example, in agriculture, biomedicine, paper making, removal of different types of dyes and heavy metal ions from wastewater, composite matrix, and food industries[1-5].

However, these applications and the effectiveness of the two biopolymers were shown to depend mainly on both the degrees of acetylation (DA) and deacetylation (DD) of chitin. Several studies have focused on optimizing the parameters of extracting chitin from its natural sources followed by its deacetylation to obtain chitosan with height DD[6-12]. Although various methods can be found in the literature for the removal of proteins and minerals from the shell, detrimental effects on the DA and DD cannot be avoided with any of these extraction processes. Therefore, a

great interest still exists for the optimization of the extraction of chitin and the steps of its deacetylation to bring the DDs to a satisfactory value for specifics applications.

The process of desacetylation involves the removal of acetyl groups from the molecular chain of chitin (Fig.1), leaving behind a complete amino group ($-NH_2$) and chitosan properties are very linked on this high degree of chemical reactive amino groups. Since the degree of deacetylation depends mainly on the method of purification and reaction conditions, it is therefore essential to characterize chitosan by determining its DD prior to its use. The main parameters involved in the process are temperature, time of reactions and the concentration of reagents. A simple and non-expensive chemical treatment of mineral/protein removal from chitin are usually used with HCl/NaOH reagents respectively, and chitosan is chemically or enzymaticaly produced[13].

The goal of this work is to produce chitosan in various experimental conditions by varying the temperature and concentration of NaOH during the deacetylation of chitin extracted from the shrimp shells. The influences of these parameters on the kinetics of its deacetylation are examined.
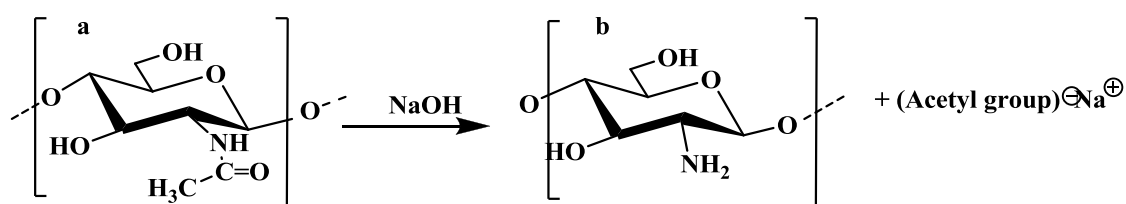

Figure 1. N-Deacetylation of chitin (a) to chitosan (b)

Results and Discussion

Characterization of SS

Prior to demineralization and deproteinization treatments; the shrimp shells were first dried at 75 °C for 24h and then characterized by FTIR. The spectrum in figure 2 shows the different bands detected. Some of these bands are attributed to different vibrations modes of CH_2, CH_3, C=O, N-H and O-H. These groups are compatible with structural units of chitin (Fig.1) and proteins, where the amide I (C=O and C-N) and amide II (1500-1700 cm^{-1}) gave two major bands in their infrared spectra. Amide II results from the N-H bending vibrations and from C-N stretching vibration. The IR spectrum of calcium carbonate was quite characteristic with a very intense broad band centred at 1435 cm^{-1} and very sharp bands at 1795, 873 and 712 cm^{-1}. These bands corresponded to the shrimp shells compositions, which was about 30-40% proteins, 30-50% calcium carbonate, 20-30% chitin and also the pigments of a lipidic nature such as carotenoids[16-18]. These proportions varied with the origin of species and with season. These FTIR identifications showed that the shrimp shells used did not contain other compounds that might result from contaminants.

Chitin extraction from SS

The FTIR spectrum of isolated chitin is shown in figure 3. The different bands observed were assigned according to the chemical structure of chitin (Fig.1) and the data in the literature[4-8,14,19,20]. The frequency of the amide I regions (between 1600 and 1660 cm^{-1}) was of great importance because it distinguished between the two structures α and β chitin. Indeed, the doublet at 1660 and 1626 cm^{-1} was assigned to νC=O and arises from the existence of two types of H-bonds or amide groups in which the C=O were involved only in α-chitin, whereas in β-

chitin these bands appeared as a single peak. The most accepted explanation was the existence of two types of amides. Half of the carbonyl groups were bonded through hydrogen bonds to the amino group inside the same chain (C=O….H-N) that was responsible for the vibration mode at 1660 cm^{-1}. Studies indicated that chitin, in the crystalline state, showed only one intense peak at 1626 cm^{-1} and the presence of these two bands in the spectrum were probably due to an amorphous state. In the region of the OH and NH groups (3600– 3000 cm^{-1}) the α-chitin exhibits a band at 3435 cm^{-1} which corresponds to the intramolecular hydrogen bond while the bands at 3256 and 3108 cm^{-1} were attributed respectively to the vibrational modes of the NH of the amide (intermolecular hydrogen bond) and the NH groups intramolecularly bonded by H. The existence of all these molecular H-bonds was responsible for the high chemical stability of the α-chitin structure. The bands located at 1420 and 1380 cm^{-1} were linked to those located in the region 2800-3000 cm^{-1}, which was attributed to the C—H stretching in CH$_3$ and CH$_2$.

Deacetylation of chitin

FTIR analysis

Two examples of the evolution of FTIR spectra over the time of deacetylation reaction of chitin, carried out in a concentrated NaOH aqueous solution (12N) at T = 120 °C and T = 25 °C, are presented respectively in figure 4: A and B. A changes in FTIR spectrum of chitin during deacetylation are noted, particulary in the domains of vibrations of amide I (1660-1620 cm^{-1}), amide II (1556 cm^{-1}) and in the region 3000-3500 cm^{-1}. For the time t < 120 min of deacetylation reaction, an intensification of all bands occurs and as the alkali treatment time increases, they decrease with significant modifications, especially in the case of T = 120 °C (Fig. 4A). These behaviors can be explained by a significant removal of acetyl group (1660 and 1626 cm^{-1}: Amide I) as confirmed by the formation of a new band at 1600 cm^{-1} assigned to the deformation of – NH$_2$ which means that the product obtained is chitosan[4-7,20,21]. Indeed, the amide I band, which is initially split into two peaks in α-chitin (fig.3), significantly weakens and turns progressively into one peak, indicating a losing of both acetyl groups and hydrogen bonds. In the region (3000-3400) cm^{-1}, the peaks at 3256 cm^{-1} and 3108 cm^{-1}, assigned to the intermolecular C=O---H–N and intramolecular H bonded NH groups in the α-chitin became in the form of small shoulder after t = 180 min or concealed, which suggests the decrease of both of these two types of hydrogen bonds and corroborates the evolution noted in the region (1660-1620) cm^{-1}.
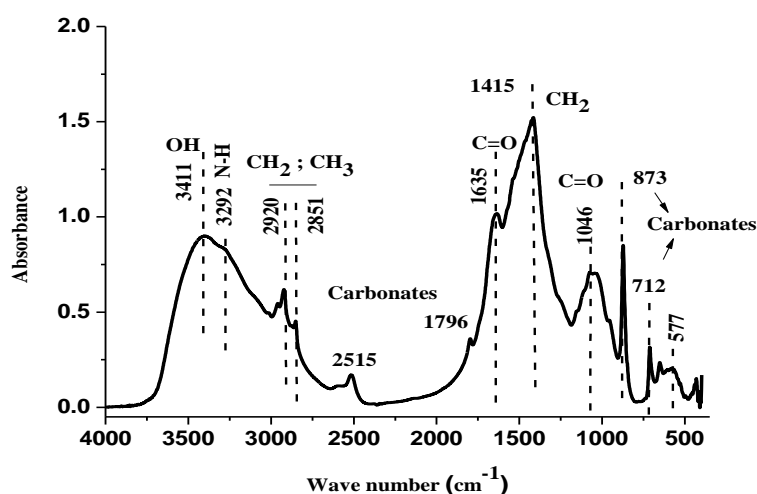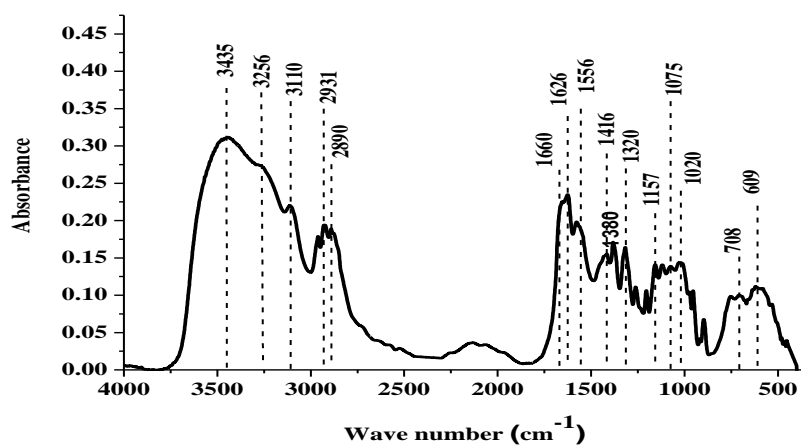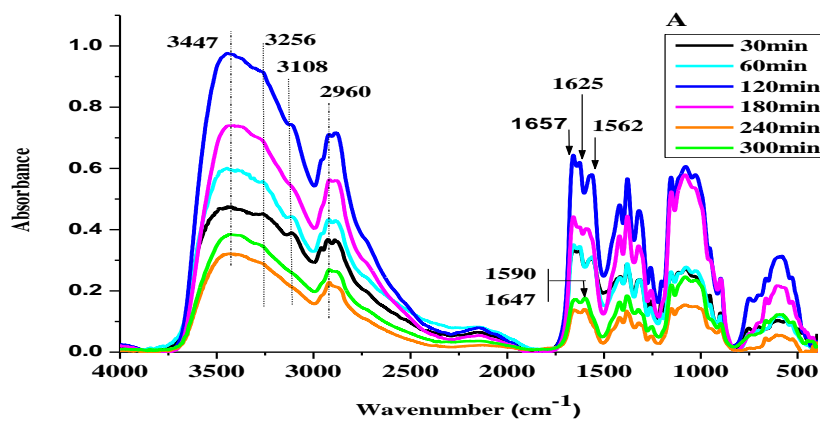

Figure 2. FTIR spectrum of SS

Figure 3. FTIR spectrum of a-chitin exacted from SS

Spectrum of α-chitin exacted from

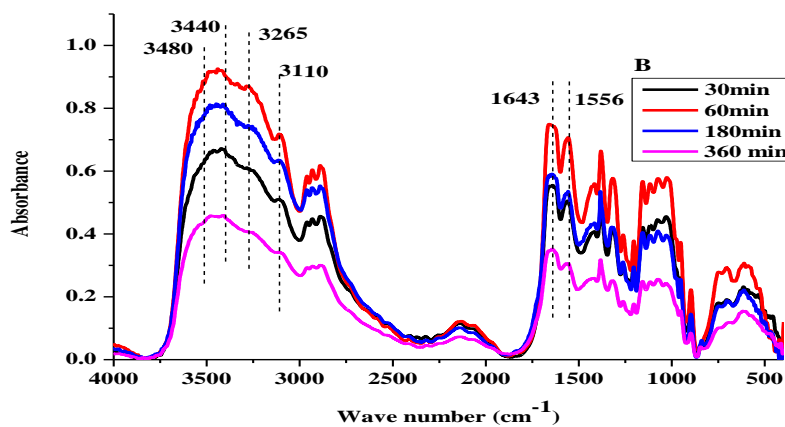**Figure 4. FTIR spectra of chitin samples taken at different times of the deacetylation reaction at T = 25 °C and T = 120 °C using C_{NaOH} = 12 N**

However, FTIR spectra in figure.4B representing samples obtained from the deacetylation of chitin with NaOH 12N at 25° C, exhibited slight changes, compared with previous deacetylated at 120 ° C. It can be seen, even at long time of alkali treatment t > 60 min that the two bands at 1660 and 1625 cm^{-1} (Amide I) overlapped to give a single flat peak centered at 1643 cm^{-1}, while that of the amide II (1556 cm^{-1}) had not gone, indicating a slower deacetylation at 25 °C. These differences showed that the temperature had a significant effect on deacetylation of chitin at the same alkaline concentration. The band in the region 3500 – 3100 cm^{-1} stayed in their initial positions and became broad, indicating a partially losing of both acetyl groups and strong intra/inter hydrogen bonds (hydrogen bonds O-6-H---O=C and O-3-H---O-5 occur at 3480 cm^{-1} and 3440 cm^{-1}), respectively. The latter became in the form of sharp band in spectra recorded at T = 120 °C, confirming the breaking of H-bond. These effects were confirmed by the DD values calculated for these reactions. As determined from FTIR spectra (Fig.4: A and B) with equation 1, it was found that DDs = 71% and 55% for chitin treated during 6h with NaOH (12N), respectively at 120 °C and 25 °C. It may be assumed[22, 23], in the single step alkaline treatment, that the increase of DD might be due to morphological changes and loose arrangement of chitin molecules, induced at height temperature and prolonged reaction times treatment, facilitating the accessibility of acetyl groups in chitin.

XRD characterization

The diffractograms of α-chitin and α-chitin treated at 120 °C with NaOH(12N) for 2h and 3h, exhibited two major crystalline peaks located at 2θ = 9.52 and 19.42 (Fig.5) with minor peaks, in accordance with published data[7,13,21,23-25]. These peaks were attributed respectively to the GlcNAc (acetyl-glucosamine) and GlcN (glucosamine) sequences in chitin (Fig.1), and the plans reflections [020] and [110], which confirmed the partial crystallinity of the polymers. It was noted that, after deacetylation process for 3h, the intensities of these peaks increased and moved slightly to a lower angle. The results indicated that there were expansions of d spacing from d = 9.27 Å to d = 9,35 Å and from d = 4.58 Å to d = 4.62 Å for [020] and [110] reflections respectively, of the crystal structure due to the change of contents of acetyl groups and H-bonds in chitin during its deacetylation. In their calculations of the d-spacing change of the (020) plane, Zhang et al[24,25] found that at around half DD there were more expansions of the crystal lattices than that of lower or higher DD. For reaction time t = 3h, the FTIR spectrum (Fig.4) showed a change of amide I and Amide II bands giving a DD = 58% that confirmed the XRD observations.
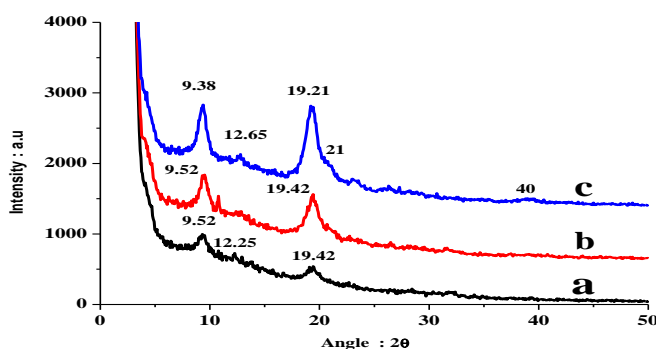
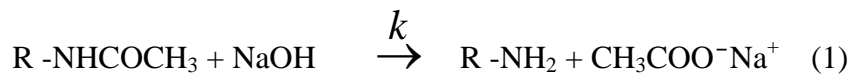**Figure.5. XRD patterns of α-chitin under various times of deacetylation at T= 120 °C and C_{NaOH} = 12 N: a : chitin (t = 0 h); b: t = 2 h and c: t = 3 h**

1   **Kinetics of deacetylation of chitin**
2   The α-chitin sample thus obtained was deacetylated at different temperatures for various
3   concentrations C_{NaOH} and time of the reaction (1):

4           $$R\text{-}NHCOCH_3 + NaOH \xrightarrow{k} R\text{-}NH_2 + CH_3COO^-Na^+ \quad (1)$$
5
6   The rate of disappearance of acetyl groups is given by the following equation: - $dN/dt = k.N$.

7
8   Assuming the concentration of C_{NaOH} constant, the apparent reaction rate constant can be
9   written as: $k = A.exp\left(-Ea/_{R.T}\right)C_{NaOH}$ (2), where $N = (N_0\text{-}X)$ and X are the numbers of
10   acetyl and amino groups contained in the chitin and chitosan, respectively, at time t of
11   reaction. After integration between initial time $t = 0$; N_0 and t ; N, we obtain:

12
13           $$-ln\frac{(N_0 - X)}{N_0} = -ln(1 - DD) = k.t \quad (3)$$

14   The ratio X/N_0, expresses the DD which is the mole fraction of deacetylated units in the
15   biopolymer chain.

16
17   **Kinetic of deacetylation at T = 25 °C**
18   The values of DDs, determined from FTIR spectra (Fig.4B), are fitted over time for
19   various concentrations of NaOH, are shown in figure 6. For $C_{NaOH} = 12N$, the DDs do not
20   exceed 55% and leveled off after a critical time t < 60 min. For less concentrated NaOH the
21   critical time became higher, indicating that the rate of the reaction of deacetylation is low
22   which means that the deacetylation is highly dependent on the concentration of NaOH,
23   because of the inaccessibility of acetamide groups in the polymer chain. These kinds of
24   behavior, observed by other authors, are explained firstly by the fact that the N-deacetylation
25   occurs preferably at the amorphous region of chitin, then proceeds from the edge to the inside
26   of the crystalline region[26,27]. The second reason is concerned about the equilibrium of the
27   deacetylation reaction and the degradation of chitosan. Other authors[10,22,28], have assumed
28   that it may be controlled both by reaction and diffusion. The low deacetylation of chitin was
29   also ascribed to the trans-arrangement of acetyl groups in the monomeric unit with respect to
30   the hydroxyl group OH[9].

31
32   **Kinetics of deacetylation at T = 80 °C and T = 120 °C**
33   Curves in figure 7A and 7B show that the DDs increase as the NaOH concentration and
34   temperature increases as the time of reaction increases. These reached a maximum of 63%
35   and 71% for $C_{NaOH} = 12N$ at $T = 80$ °C and 120 °C respectively. On the other hand, it can be
36   observed that the critical time decreases when the temperature and the concentration of
37   NaOH increase. Consequently, at the beginning of the treatment, a fast and easy
38   desacetylation occurs, followed by a plateau which reveals a second step of deacetylation like
39   the trend observed at $T = 25$ °C (Fig.6). It can be seen in the case of $C_{NaOH} = 12N$ and $T =$
40   120 °C, the deacetylation continues for a longer time and tends also towards an asymptote.
41   The augmentation of DDs values with these parameters can be attributed to the change of the
42   structure during deacetylation of chitin at height temperature, as confirmed by FTIR and
43   XRD studies.

1   In the mechanism of the deacetylation of chitin, the second step is mainly explained by
2   the diffusion, the equilibrium reaction and the inaccessibility of reagents to the amorphous
3   region. Recently, under solid–liquid phase transfer catalysis, Sarhan et al[28], proposed a
4   mechanism where the heterogeneous N-deacetylation is controlled by both reaction and
5   diffusion: The first step involves the reaction of the onium salt, designated as (Q^+X^-), with
6   NaOH to give the corresponding onium hydroxide (Q^+OH^-) which is able to diffuse from the
7   aqueous to the organic phase to start the deacetylation process by attacking the C=O of the
8   acetyl group, then after the completion of the hydrolysis reaction, the resulted onium acetate
9   ($CH_3COO^-Q^+$) will diffuse to the aqueous phase to be regenerated to a new onium hydroxide
10 through the reaction with NaOH. From our results, at longer time of deacetylation, the ratios
11 DDs/C_{NaOH} remain constant at each temperature, which means that the deacetylation reaction
12 reached equilibrium.
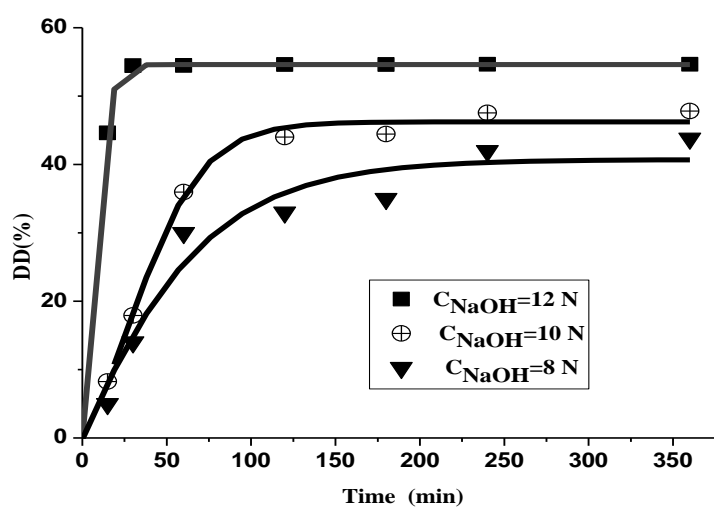
13
14   **Figure 6. Evolution at 25 °C of the DD% as a function of the reaction time and**
15   **C_{NaOH}**

16
17
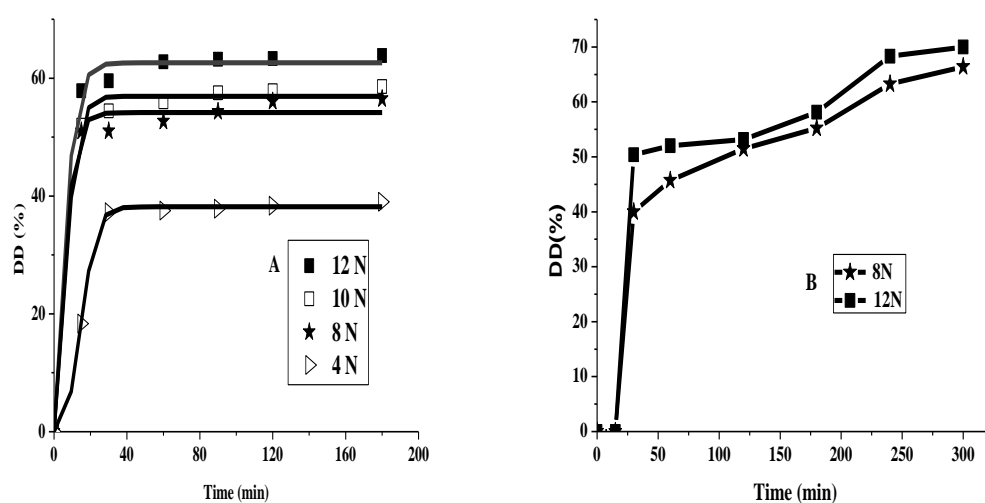
18   **Figure 7. Evolution at 80 °C (A) and 120 °C (B) of the DD% as a function of the**
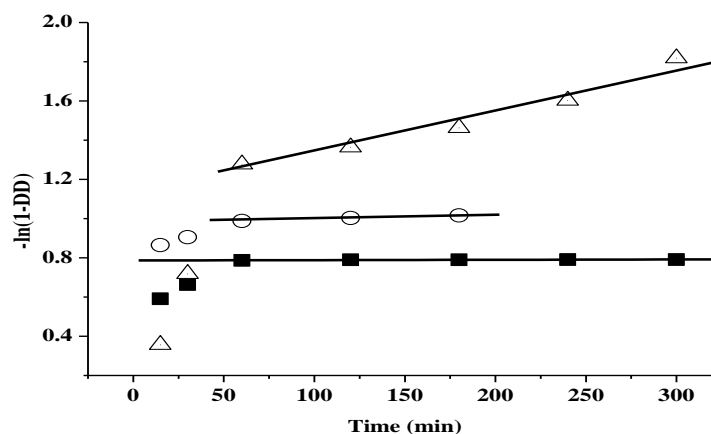19   **reaction time and C_{NaOH}**

1
2
3

Determination of apparent rate constant k and activation energy Ea:

4 k is determined by plotting the equation 3. Considering the second step, it can be observed
5 (Fig.8), for all temperatures studied (25 °C, 80 °C and 120 °C) at the same alkaline
6 concentration (12N), the deacetylation process followed the pseudo-first order kinetics. Tab.1
7 shows that the values of k derived from the slope of straight line obtained are very low,
8 reflecting the existence of a limiting step. These values declined as a function of temperature
9 decreased. This indicates that the rate of deacetylation reaction is faster at the beginning of
10 the reaction t < 60 min, but at the subsequently times it was very slow.

11
12

Table 1: Apparent rate constant

T(°C)	25	80	120
k_2 (min^{-1}) 2nd step	1.70×10^{-5}	2.23×10^{-4}	22×10^{-4}

13

14 The apparent activation energy was estimated as about 48.76 kJ/mol from the straight line
15 of the Arrhenius plot (ln k vs (1/T)) shown in figure 9. This value is in the same order of
16 magnitude as those found by other authors for heterogeneous N-deacetylation performed
17 between 80 °C and 120 °C[8,10,12,22,26]. The results indicated that the reaction at higher
18 concentration and temperature proceeded easier than that at their lower values.

19
20 **Figure 8. -ln(1-DD) versus the time of deacetylation reaction at different**
21 **temperature and C_{NaOH} = 12N**

Y = 8,56931 - 5865,01141.X
R^2 = 0,9913
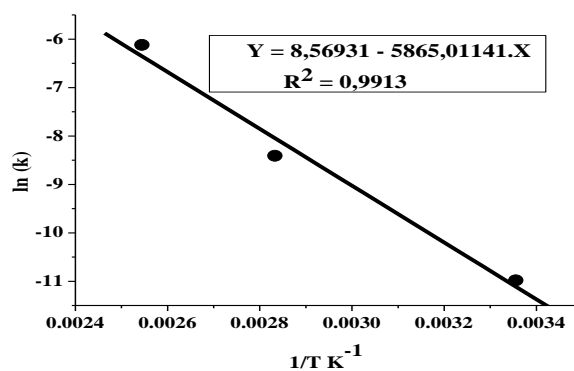
22
23 **Figure 9. The Arrhenius plot of ln(k) vs. 1/T.**

Conclusion

α-chitin extracted from shrimp shells collected in the city of Meknes in Morocco was deacetylated at the optimal experimental condition: T = 120 ° C, C_{NaOH} = 12N and t = 300 min, to obtain a high DD (76%). The deacetylation reaction occurs in two stages with different rate constants obeying a first-order kinetics. The apparent activation energy was estimated to be 48.76 kJ/mol, in the temperature range of 25 °C – 120 °C, which was in good agreement with the published data. It means that the N-deacetylation of chitin is less reactive in the second step of reaction. This may be due to the equilibrium reaction, diffusion or the inaccessibility of acetyl group as described in the cited literature. FTIR and XRD technique confirms the change of the structure of chitin during its deacetylation.

Experimental Section

Material

The raw material that was used along this study is the shell of shrimp (SS) collected from restaurants and fishmongers in the city of Meknes (Morocco). These shells were first removed from their antennas and legs and then washed thoroughly with tap water followed by distilled water until no contamination is present on the shells. Before use, they were dried at 75 °C for 24h and then milled in a hammer mill through a fine particle. All others reagents used: NaOH pellets, HCl and CH_3CO_2H, were analytical grade.

Chitin extraction

A mass m = 1g of dry shells was mixed with 15 ml of concentrated aqueous solutions of HCl (1N) at room temperature and then stirred vigorously for 24h. The demineralised shells were filtered and deproteinized with 15 ml of sodium hydroxide (1N) for 24h at room temperature under vigorous stirring. These procedures were repeated three times to dissolve all the minerals and the proteins parts. The sample obtained, which is the final chitin, was washed thoroughly with deionised water until absence of chloride (confirmed by the $AgNO_3$ test) and reaching neutral pH. The sample was dried in an oven at T = 75 °C for 5h and then stored for future use.

Chitosan preparation: deacetylation of chitin

Chitosan is obtained by hydrolysis of acetyl groups contained in chitin by a concentrated aqueous solution of NaOH. The reaction of deacetylation was carried out with concentrations of NaOH equal to 8N, 10N and 12N. For each of these concentrations, the kinetics of deacetylation were studied at different temperatures (25 °C, 80 °C and 120 °C) for treatment times varying between 30 to 300 min in a reflux reactor. After a desired interval time, the samples were filtered in order to separate the supernatant from the solid fraction which is the chitosan. The latter was extensively washed with deionised water until pH = 7 and dried at 80 °C overnight. The chitosan obtained was in a white colour. Both fractions (soluble and insoluble) were then kept in a freezer for further characterizations. The solid/liquid ratio was kept constant along these experiments to 1/15 w/v.

1 **Characterization of samples**

2

3   **FTIR spectroscopy**

4   The Fourier Transform Infrared Spectrometer spectra (400–4000 cm^{-1}) were registered in
5   absorption frequencies in an FTIR (shimadzu, JASCO 4100) connected to a PC with software
6   for data processing. The samples were prepared in KBr discs in the usual way from very well
7   dried mixtures of about 4 % (w/w) and stored in a desiccator. The spectra were obtained with
8   4 cm^{-1} resolution and 64 scans. This technique is often applied for determination of the DD
9   because of its simplicity. For this different absorption band, ratios had been already
10 proposed[6,8,13-15]. However, choosing an appropriate calculation procedure was not an easy
11 task since the choice of the baseline on IR spectra, reference, and the probe bands were
12 difficult. In this work, the average DD was determined by the following formula, usually
13 used:

14
$$DD(\%) = 100 - \left[\frac{A_{1665}}{A_{3450}} \times \frac{100}{1.33} \right] \qquad (1)$$

15 where A_{1655} is the absorbance at 1655 cm^{-1} of the amide I band as a measure of the N-acetyl
16 group content and A_{3430} is the absorbance at 3430 cm^{-1} due to hydroxyl group as an internal
17 standard. The value 1.33 represents the ratio of these absorbance for fully acetylated
18 compound. An appropriate baseline in each spectrum was determined by using origin
19 software.
20

21 **X-ray analysis**

22 The X-ray diffraction (XRD) patterns was obtained using a X'PERT MPD-PRO wide
23 angle X-ray powder diffractometer provided with a diffracted beam monochromator and Ni
24 filtred CuKα radiation (λ = 1.5406 Å). The voltage was 45 kV and the intensity 40 mA. The
25 2θ angle was scanned between 4° and 60°, and the counting time was 2.0 s at each angle step
26 (0.02°). XRD analysis was applied to detect the crystallinity of the extracted sample of chitin
27 and their corresponding chitosan.

28

29 **References**

30

31 1. S. Bautista-Banõs, A.N. Hernández-Lauzardo, M.G. Velázquez-del Valle, M. Hernández-
32   López, E. Ait Barka, E. Bosquez-Molina, C.L. Wilson, Crop Protection, **2006**, 25, 108–
33   118.
34 2. Z. Cao, Z. H. Ge, S. Lai, European Polymer Journal, **2001**, 37, 2141-2143.
35 3. M. Valentina Dinu, E. Stela Dragan, Chemical Engineering Journal, **2010**, 160, 157–163.
36 4. M. Rinaudo, Progress in Polymer Science, **2006**, 31, 603–632.
37 5. J. Iqbal, F.H. Wattoo, M.H. Sarwar Wattoo, R. Malik, S.A. Tirmizi, M. Imran, A.B.
38   Ghangro, Arabian Journal of Chemistry, **2011**, 4, 389–395.
39 6. M.R. Kasaai, Carbohydrate Polymers, **2008**, 71, 497–508.
40 7. F.A. Al Sagheer, M.A. Al-Sughayer, S. Muslim, M.Z. Elsabee, Carbohydrate Polymers,
41   **2009**, 77, 410–419.
42 8. M.L. Duarte, M.C. Ferreira, M.R. Marvão, J. Rocha, International Journal of Biological
43   Macromolecules, **2002**, 31, 1- 8.
44 9. A. Tolaimate, J. Desbrières, M. Rhazi, A. Alagui, M. Vincendon, P. Vottero, Polymer,
45   **2000**, 41, 2463–2469.

10. P. Methacanon, M. Prasitsilp, T. Pothsree, J. Pattaraarchachai, Carbohydrate Polymers, **2003**, 52, 119–123.

11. A. Chandumpai, N. Singhpibulporn, D. Faroongsarng, P. Sornprasit, Carbohydrate Polymers, **2004**, 58, 467–474.

12. G. Galed, B. Miralles, I. Panõs, A. Santiago, Á. Heras, Carbohydrate Polymers, **2005**, 62, 316–320.

13. D. Ren, H. Yi, W. Wang, M. Xiaojun, Carbohydrate Research, **2005**, 340, 2403–2410.

14. J. Brugnerotto, J. Lizardi, F.M. Goycoolea, W. ArguÈelles-Monal, J. Desbrie Áres, M. Rinaudo, Polymer, **2001**, 42, 3569 – 3580.

15. D. Baskar, T.S. Sampath Kumar, Carbohydrate Polymers, **2009**, 78, 767–772.

16. W. Sajomsang, P. Gonil, Materials Science and Engineering C, **2010**, 30, 357–363.

17. A. Percot, C. Viton, A. Domard, Biomacromolecules, **2003**, 4, 1380-1385.

18. G. Chaussard, D. Domard, Biomacromolecules, **2004**, 5, 559-564.

19. T.G. Liu, B. Li, W. Huang, B. Lv, J. Chen, J.X. Zhang, L.P. Zhu, Carbohydrate polymers, **2009**, 77, 110–117.

20. R.L. Lavall, O.B.G. Assis, S.P. Campana-Filho, Bioresource Technology, **2007**, 98, 2465–2472.

21. M. Fan, Q. Hu, K. Shen, Carbohydrate Polymers, **2009**, 78, 66–71.

22. N. Yaghobi, F. Hormozi, Carbohydrate Polymers, **2010**, 81, 892–896.

23. T. Lertwattanaseri, N. Ichikawa, T. Mizoguchi, Y. Tanaka, S. Chirachanchai, Carbohydrate Research, **2009**, 344, 331–335.

24. Y. Zhang, C. Xue, Y. Xue, R. Gao, X. Zhang, Carbohydrate Research, **2005**, 340, 1914–1917.

25. Y. Zhang, C. Xue, Z. Li, Y. Zhang, X. Fu, Carbohydrate Polymers, **2006**, 65, 229–234.

26. K. Kurita, T. Sannan, Y. Iwakura, Makromolekulare Chemie, **1977**, 178, 3197–3202.

27. T. Sannan, K. Kurita, Y. Iwakura, Polymer Journal, **1977**, 9, 649-651.

28. A.A. Sarhan, D.M. Ayad, D.S. Badawy, M. Monier, Reactive & Functional Polymers, **2009**, 69, 358